Energy & Environmental Science

Cite this: *Energy Environ. Sci.*, 2012, **5**, 8538

www.rsc.org/ees

COMMUNICATION

Three-dimensionally ordered macroporous FeF_3 and its *in situ* homogenous polymerization coating for high energy and power density lithium ion batteries†

De-long Ma,[ac] Zhan-yi Cao,[c] Heng-guo Wang,[a] Xiao-lei Huang,[ab] Li-min Wang[a] and Xin-bo Zhang*[a]

Received 16th June 2012, Accepted 17th July 2012
DOI: 10.1039/c2ee22568a

A new hybrid nanostructure composed of three-dimensionally ordered macroporous (3DOM) FeF_3 and an homogenous coating of poly(3, 4-ethylenedioxythiophene) (PEDOT) is successfully synthesized using polystyrene (PS) colloidal crystals as hard template, and the coating of PEDOT is achieved through a novel *in situ* polymerization method. The special nanostructure provides a three-dimensional, continuous, and fast electronic and ionic path in the electrode. Surprisingly, the advantageous combination of 3DOM structure and homogenous coating of PEDOT endows the as-prepared hybrid nanostructures with a stable and high reversible discharge capacity up to 210 mA h g^{-1} above 2.0 V at room temperature (RT), and a good rate capability of 120 mA h g^{-1} at a high current density of 1 A g^{-1}, which opens up new opportunities in the development of high performance next-generation lithium-ion batteries (LIBs).

The past two decades have witnessed lithium-ion batteries (LIBs) successfully capture the portable electronic market. However, if they are proposed to conquer the upcoming markets of electric vehicles, storage of energy from renewable sources and load-leveling, great improvements in storage capacity (which is currently mainly limited by their electrode materials, especially at the cathode side) are urgently needed.[1] The solution to this requires a new concept to break through the limitation of one-electron redox chemistry ($1e^-$ per 3d metal) as occurs for classical Li insertion/deinsertion reactions.[2] To this end, inspired by the pioneering work of Tarascon and coworkers, intensive researches have been devoted to various conversion reaction compounds, such as metal oxide, hydroxide, hydride, sulfides, and fluorides, *etc.*[3] Among them, compared with the numerous researches and significant improvements in anodes, there is little report on cathodes. Therefore, the development of high-capacity conversion-based cathode materials to improve simultaneously the energy and power density is of great importance but still very challenging.

Metal fluorides, as one of the most important families of functional inorganic materials, have numerous applications in the fields of catalysts, optical devices and magnetic materials. Among them, iron trifluoride (FeF_3) is considered as a promising conversion-based cathode material due to its high operating potential, high theoretical capacity of 237 mA h g^{-1} ($1e^-$ transfer) and 712 mA h g^{-1} ($3e^-$ transfer), low cost, abundant sources, and better safety.[4] However, its implementation in LIBs is greatly hindered by its poor power performance, which is seriously limited by the slow diffusion of lithium ions and low conductivity of FeF_3 and LiF (the product of the conversion reaction), and poor cycle stability, which might be due to the drastic volume variation during the Li uptake-and-release process. To circumvent these obstacles, many strategies including downsizing the electrode materials to the nanoscale through high-energy mechanical ball-milling, pulsed laser deposition, ionic-liquid assisted methods, and/or coating or mixing with more conductive materials, have been developed.[5] Despite the fact that significant improvements have been achieved, the obtained performance is still far from satisfactory and the research on FeF_3 is still in its infancy.

Contrary to small and isolated 0D spherical nanoparticles (NPs), when electroactive materials are in a 3DOM structure and successfully coated with more conductive materials, the so-obtained interconnection (immobility) and open porous structure could eliminate the problems of NPs aggregation upon cycling and structural instability against volume variation, respectively, which would theoretically benefit the cycling stability.[6] Even more importantly, the 3DOM morphology offers substantial improvement in power and energy density over bulk electrodes stemming from the structural advantages as follows. Firstly, the interconnected pores facilitate the transport and infiltration of electrolyte and thus would offer sufficient contact interface between active materials and electrolyte. Secondly, the thin wall and porous structure shorten both the electronic and ionic pathways within the particles. Thirdly, the interconnection structure and the homogenous coating of more conductive materials provide a three-dimensional, continuous, and fast electronic path in the electrode, which allows faster charge transport.[7] To the best of our knowledge, there is no report on 3DOM FeF_3, to say nothing of those with a homogenous conducting polymer coating. As a result, it

[a]*State Key Laboratory of Rare Earth Resource Utilization, Changchun Institute of Applied Chemistry, Chinese Academy of Sciences, Changchun 130022, China. E-mail: xbzhang@ciac.jl.cn; Fax: +86-431-85262235; Tel: +86-431-85262235*
[b]*Graduate University of Chinese Academy of Sciences, Beijing 100049, China*
[c]*Key Laboratory of Automobile Materials, Ministry of Education, School of Materials Science and Engineering, Jilin University, Changchun 130012, China*

† Electronic supplementary information (ESI) available. See DOI: 10.1039/c2ee22568a

remains unexplored but highly desirable to develop a facile and effective strategy to synthesize 3DOM FeF_3 toward superior lithium storage capacity, cycling and rate performance.

Herein, we first report the fabrication of a new hybrid nanostructure composed of 3DOM FeF_3 with a homogenous coating of PEDOT, and its superior electrochemical lithium storage performance. The 3DOM FeF_3 is fabricated using PS colloidal crystals as hard template, and the coating of PEDOT is achieved through a novel *in situ* polymerization method, which plays a key role to ensure the homogeneity of the coating and the intimate contact between the active material (FeF_3) and the conductive agent (PEDOT), and thus fast and continuous electron transport along the 3DOM network. Furthermore, compared to the classical carbon coating technology, this novel coating approach is free of high temperature and CO_2 formation and thus is cost-efficient and environment friendly. Surprisingly, the advantageous combination of 3DOM structure and the homogenous coating of PEDOT endows the as-prepared hybrid nanostructures with a stable and high reversible discharge capacity up to 210 mA h g^{-1} above 2.0 V at RT, and good rate capability of 120 mA h g^{-1} at a high current density of 1 A g^{-1}, which opens up new opportunities in the development of high performance next-generation LIBs.

Fig. 1 schematically shows the strategy and motivation for the fabrication of the PEDOT–3DOM FeF_3 hybrid nanostructure. Briefly, the PS colloidal crystals (Fig. S2†) are first impregnated with the $FeF_3 \cdot 3H_2O$ in mixed water and methanol solution for 2 h, wherein the water and methanol mixture plays a key role in finely tuning the polarization of the solution, that is, water is used to ensure the high solubility of $FeF_3 \cdot 3H_2O$ and thus a high product yield, while the methanol is employed to ensure the high wetting property of PS and thus high efficiency of the replication process. The residual solution is then removed *via* a vacuum filter. After drying, the 3DOM $FeF_3 \cdot 3H_2O$ is obtained by dissolving PS colloidal crystals in toluene. Finally, the hydration water is removed by mild heat treatment, and the conducting polymer PEDOT is coated homogeneously on the surface of the 3DOM FeF_3 by a novel *in situ* polymerization of EDOT thanks to the intrinsic oxidation capability of FeF_3. The polymerization of EDOT follows eqn (1):

$$FeF_3 + LiTFSI + EDOT \rightarrow PEDOT + LiFeF_3 \quad (1)$$

where the lithium bis(trifluoromethanesulfonyl)imide (LITFSI) is used as lithium source since it is a stable salt under ambient conditions, and TFSI, used as the counter ion for the oxidized state of PEDOT, could give polymers with high conductivity.[8] Fig. 1 also schematically illustrates the idea and motivation, namely, the advantageous combination of the better conductivity of PEDOT and the short diffusion distance of the porous 3DOM FeF_3.

X-Ray diffraction (XRD) analysis is performed to investigate the crystal phase of the fabricated samples. All the diffraction peaks of the fabricated samples after freeze drying could be indexed to α-$FeF_3 \cdot 3H_2O$ (Fig. S1a†), which is the metastable phase for $FeF_3 \cdot 3H_2O$.[9] No other crystalline impurities are detected. After heat treatment, α-$FeF_3 \cdot 3H_2O$ loses its lattice water and becomes amorphous (Fig. S1b†). The morphology and structure of the as-prepared samples are investigated by scanning electron microscopy (SEM) and transmission electron microscopy (TEM). Fig. 2a–c show the TEM images of 3DOM FeF_3 before PEDOT coating. Interestingly, the close packing order of the original PS template (Fig. S2†) is successfully preserved after removing the PS template, highlighting the efficacy of our proposed synthesis strategy. Obviously, in each image, the dark areas correspond to the FeF_3 framework and the light areas to the void space. The well-ordered "air spheres" and interconnected 3DOM FeF_3 walls create a "honeycomb" pore structure in three dimensions. The images correspond to views along the [111] (Fig. 2a) and [011] (Fig. 2b) directions for a lattice formed by filling the interstitial spaces of a face-centered cubic array of PS. In

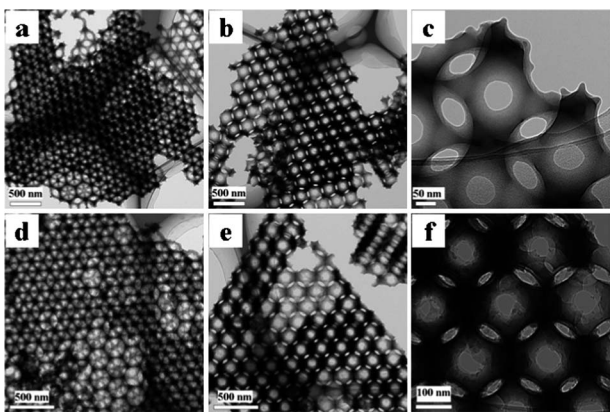

Fig. 2 TEM images of 3DOM FeF_3 before (a, b and c) and after (d, e and f) coating with PEDOT.

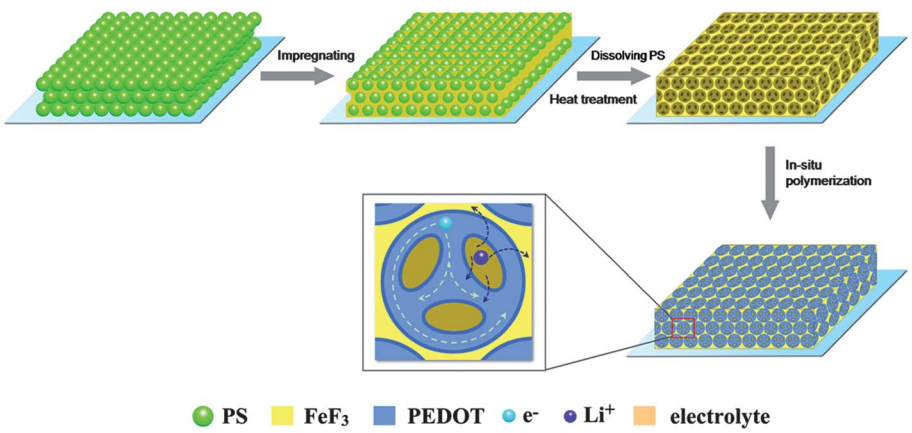

Fig. 1 Schematic illustration of the strategy and motivation of synthesis of 3DOM FeF_3 coated by PEDOT.

addition, the wall thickness of the as-prepared 3DOM FeF_3 framework is about 50–80 nm, and the diameter of the primary and secondary pore is about 250 and 20–50 nm, respectively. Interestingly, the 3DOM framework is kept almost unchanged after the polymerization of EDOT (Fig. 2d–f) while the surfaces become rather rough, indicating the successful coating of PEDOT. Furthermore, as shown in Fig. 3, the formation of PEDOT is further confirmed by the C=C ring and C–O–R vibrations at 1181 cm^{-1} and the C–S vibration at 929 cm^{-1}. The polymer p-doping is also indicated by the bands at 1514 and 1320 cm^{-1}, which is similar to the material polymerized by solution oxidants.[10] These results demonstrate that the 3DOM FeF_3 has been uniformly coated by PEDOT. Moreover, when FeF_3 is completely dissolved with diluted solution of HCl, the porous network of PEDOT can be retained (Fig. S3†), which further confirms that all the surfaces of 3DOM framework are completely and uniformly coated by PEDOT. The amount of PEDOT in the composite is *ca.* 10%, which is determined by the weight loss of PEDOT–3DOM FeF_3 after washing in HCl to remove the FeF_3.

Naturally, the open and interconnected 3DOM structures could give a high specific area to expose more surface sites. This is proved by the N_2 absorption–desorption isotherms. As shown in Fig. S4,† the sample is found to show a type-IV N_2 absorption–desorption isotherm, corresponding to a macroporous material. The pore diameter distribution is estimated by applying a Barrett–Joyner–Halenda (BJH) method to the isotherm adsorption branch (inset of Fig. S4†), and both small (<10 nm) and large pores (>25 nm) are obtained, which contribute to a relative high Brunauer–Emmett–Teller (BET) surface area of 54 $m^2\ g^{-1}$. This favorable porous structure would certainly facilitate the electrolyte diffusion and thus result in enhanced electrochemical performance (*vide infra*).

Coin cells with a metallic Li counter electrode are assembled and galvanostatic charge/discharge technique is employed to evaluate the electrochemical performance of PEODT–3DOM FeF_3 at RT. Initially, as shown in Fig. S5,† the galvanostatic charge–discharge process for PEDOT–3DOM FeF_3 is performed in a voltage range of 1.5–4.5 V with a current density of 50 mA g^{-1}. The first discharge capacity achieves 540 mA h g^{-1}, approximately corresponding to the insertion of 2.3 Li per formula, which is more than three times higher than the gravimetric capacity of the state-of-the-art cathode materials

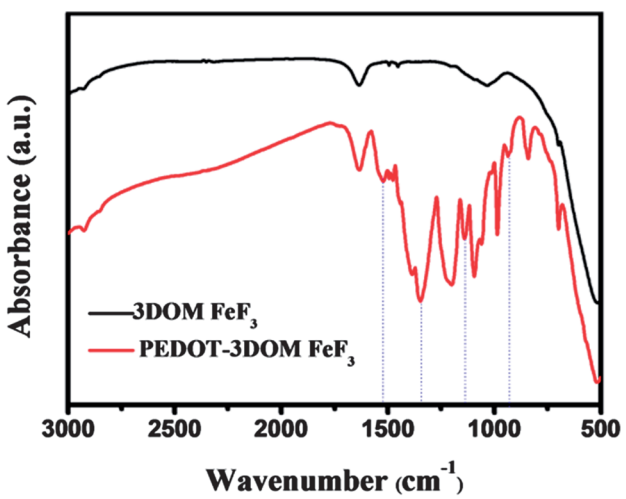

Fig. 3 FTIR of FeF_3 (black line) and PEDOT–FeF_3 (red line).

(normally less than 200 mA h g^{-1}) and thus greatly expands the range of cathode choices. Note that, the capacity is calculated based on the FeF_3–PEDOT, not just the weight of pristine FeF_3. Clearly, the discharge profile can be divided into two parts. The initial sloped area between 3.5 and 1.7 V stems from the Li^+ insertion into the FeF_3 framework *via* a two-phase reaction to form $Li_{0.5}FeF_3$ and then *via* a single-phase reaction to form $LiFeF_3$ ($FeF_3 + Li^+ + e^- \rightleftharpoons LiFeF_3$). This is followed by a reaction plateau at 1.7 V, which is due to the decomposition of formed $LiFeF_3$ to LiF and Fe metal through a conversion reaction ($LiFeF_3 + 2Li^+ + 2e^- \rightleftharpoons Fe + 3LiF$).[11a] On the contrary, during charging, no obvious plateau is observed. Such behavior is similar to that reported by Badway *et al.*[11b–d] However, the detailed reaction mechanisms remain controversial because a series of intermediates may be formed during the reaction. A cyclic voltammogram (CV) curve is employed to clarify the energy storage redox mechanism of PEDOT–3DOM FeF_3 (Fig. S6†). It should be noted that the potential difference between the cathodic and anodic peaks of latter reaction is about 1.1 V (cathodic peak: ~1.7 V; anodic peak: ~2.8 V). This huge potential hysteresis caused by polarization will induce a large energy loss during battery operation. In view of this, we chose the potential window to be from 2.0 to 4.5 V to ensure that only the insertion reaction takes place, which is facile and fully reversible. Interestingly, as shown in Fig. 4, the potential difference between the cathodic and anodic peaks of PEDOT–3DOM FeF_3 is only about 0.3 V (cathodic peak: ~3 V; anodic peak: ~3.3 V). At a current density of 20 mA g^{-1}, the discharge capacity of PEDOT–3DOM FeF_3 reaches 210 mA h g^{-1} (Fig. 4a, trace A), corresponding to an insertion of 0.88 Li per formula, which is much better than those of 3DOM FeF_3 without a PEDOT coating (Fig. 4a, trace B) and commercial nonporous FeF_3 with a PEDOT coating (Fig. 4a, trace C). For example, the capacity of 3DOM FeF_3 without a conducting PEDOT coating is only 148 mA h g^{-1} with a large polarization, which is mainly caused by the low conductivity of the pristine FeF_3. However, the conductivity is not the only key factor. When the commercial nonporous FeF_3 (without 3DOM structure) is coated by conducting PEDOT, only an even-lower capacity of 105 mA h g^{-1} can be achieved. All the above results indicate that both the 3DOM structure and the PEDOT coating play a key role in improving the electrochemical performance of FeF_3, which can ensure simultaneously fast Li-ion and electron transportation.

In addition, the PEDOT–3DOM FeF_3 shows good cycling stability. After 30 cycles under a current density of 20 mA g^{-1}, the nanocomposites still retain a reversible capacity of about 190 mA h g^{-1} (Fig. 4b). Furthermore, to examine the rate capability of PEDOT–3DOM FeF_3, the current density is increased from 50 to 3000 mA g^{-1} (Fig. 4c). Interestingly, it can deliver 170 mA h g^{-1} at a current density of 150 mA g^{-1}. Even under a high current density of 1000 mA g^{-1}, a high capacity of 120 mA h g^{-1} with low polarization can still be obtained. These results indicate that the unique hybrid nanostructures we designed are also suitable for fast charging and discharging. The enhanced electrochemical activity can be mainly attributed to the synergistic effect of the 3DOM structure and conductive surface coating, highlighting again the power and efficacy of our strategy.

As LIBs to deliver high power, the Joule effect must be considered because large amount of heat can be generated during the charge–discharge process at high power. This would heat up the battery and lead to a serious increase of the cell temperature. Meanwhile, it is also crucial to study the behavior of LIBs working at a low temperature as this is necessary for real, practical applications. Therefore, it is

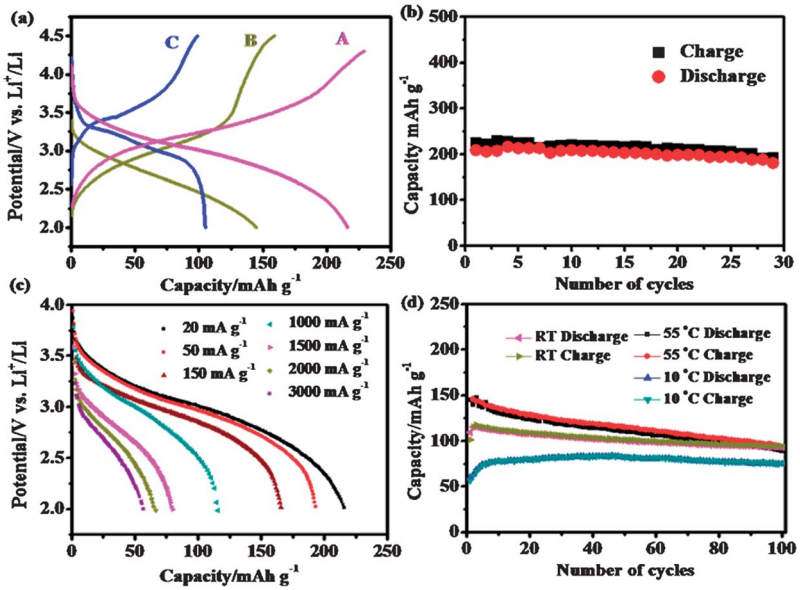

Fig. 4 (a) Charge–discharge profiles of the PEDOT–3DOM FeF_3 (A), 3DOM FeF_3 without coating (B), and commercial FeF_3 coated by PEDOT (C) at a current density of 20 mA g^{-1}. (b) Cycling stability of PEDOT–3DOM with a voltage range of 2.0–4.5 V at a current density of 20 mA g^{-1}. (c) Discharge profiles of PEDOT–3DOM FeF_3 at different current densities. (d) The cycling performance of PEDOT–3DOM FeF_3 electrode at a high current density of 1000 mA g^{-1} at 10, RT, and 55 °C.

essential to study the temperature-dependent performance. Measurements are carried out at 10 °C, RT, and 55 °C (Fig. 4d). At low temperature of 10 °C, the cell can still deliverer a capacity of 90 mA h g^{-1} even at a high current density of 1000 mA g^{-1} and, more importantly, no obvious capacity degradation is observed after 100 cycles, which is very favorable for LIBs working at low temperature. On the other hand, when temperature increase to 55 °C, a higher discharge capacity of 145 mA h g^{-1} could be achieved, which is due to the reduced resistance of the cell and enhanced ion mobility in the electrolyte at elevated temperature. However, the cycling stability decreased slightly, which might be caused by the decomposition of the electrode/electrolyte interface and the decomposition of the electrolyte promoted by the higher temperature.[12] Further research work focusing on improving the high temperature cycling stability is in progress.

In summary, a novel hierarchical structure of 3DOM FeF_3 coated with PEDOT has been successfully fabricated by a facile, scalable, yet effective method. Interestingly, the as-prepared PEDOT–3DOM FeF_3 achieves a high capacity of 210 mA h g^{-1} at a current density of 20 mA g^{-1}, and high power capability of 120 mA h g^{-1} at a current density of 1 A g^{-1} at room temperature, which could be reasonably attributed to enhance the ionic and electronic transport in the electrode, stemming from the synergistic effect of the unique 3DOM structure and the complete and uniform surface conductive coating of PEDOT. The obtained encouraging results would open up new and exciting opportunities to promote long-term endeavors in developing high capacity cathodes for rechargeable LIBs.

Acknowledgements

This work is financially supported by the 100 Talents Programme of The Chinese Academy of Sciences, the National Program on Key Basic Research Project of China (973 Program, Grant no. 2012CB215500), the Foundation for Innovative Research Groups of the National Natural Science Foundation of China (Grant no. 20921002), the National Natural Science Foundation of China (Grant no. 21101147), and the Jilin Province Science and Technology Development Program (Grant no. 20100102 and 20116008).

Notes and references

1 (*a*) J. Tarascon and M. Armand, *Nature*, 2001, **359**, 367; (*b*) K. Kang, Y. S. Meng, J. Bréger, C. P. Grey and G. Ceder, *Science*, 2006, **311**, 977.
2 P. Poizot, S. Laruelle, S. Grugeon, L. Dupont and J. Tarascon, *Nature*, 2000, **407**, 496.
3 (*a*) W. Y. Li, L. N. Xu and J. Chen, *Adv. Funct. Mater.*, 2005, **15**, 851; (*b*) J. Liu, Y. Li, X. Huang, G. Li and Z. Li, *Adv. Funct. Mater.*, 2008, **18**, 1448; (*c*) Y. Oumellal, A. Rougier, G. Nazri, J. Tarascon and L. Aymard, *Nat. Mater.*, 2008, **7**, 916; (*d*) T. J. Kim, C. Kim, D. Son, M. Choi and B. Park, *J. Power Sources*, 2007, **167**, 529; (*e*) H. Li, G. Richter and J. Maier, *Adv. Mater.*, 2003, **15**, 736; (*f*) H. Li, P. Balaya and J. Maier, *J. Electrochem. Soc.*, 2004, **151**, A1878.
4 (*a*) R. Prakash, A. K. Mishra, A. Roth, C. Kubel, T. Scherer, M. Ghafari, H. Hahn and M. Fichtner, *J. Mater. Chem.*, 2010, **20**, 1871; (*b*) P. Liao, B. L. MacDonald, R. A. Dunlap and J. R. Dahn, *Chem. Mater.*, 2008, **20**, 454; (*c*) C. Li, L. Gu, J. Tong, S. Tsukimoto and J. Maier, *Adv. Funct. Mater.*, 2011, **21**, 1391; (*d*) M. Zhou, L. Zhao, T. Doi, S. Okada and J. Yamaki, *J. Power Sources*, 2010, **195**, 4952; (*e*) N. Yabuuchi, M. Sugano, Y. Yamakawa, I. Nakai, K. Sakamoto, H. Muramatsu and S. Komaba, *J. Mater. Chem.*, 2011, **21**, 10035.
5 (*a*) F. Badway, F. Cosandey, N. Pereira and G. Amatucci, *J. Electrochem. Soc.*, 2003, **150**, A1318; (*b*) C. Li, L. Gu, S. Tsukimoto, P. A. van Aken and J. Maier, *Adv. Mater.*, 2010, **22**, 3650; (*c*) C. Li, L. Gu, J. Tong and J. Maier, *ACS Nano*, 2011, **5**, 2930; (*d*) S. W. Kim, D. H. Seo, H. Gwon, J. Kim and K. Kang, *Adv. Mater.*, 2010, **22**, 5260.
6 (*a*) F. F. Cao, Y. G. Guo, S. F. Zheng, X. L. Wu, L. Y. Jiang, R. R. Bi, L. J. Wan and J. Maier, *Chem. Mater.*, 2010, **22**, 1908; (*b*) A. S. Aricò, P. Bruce, B. Scrosati, J. M. Tarascon and W. Van Schalkwijk, *Nat. Mater.*, 2005, **4**, 366; (*c*) J. Liu, J. S. Chen, X. Wei, X. W. Lou and X. W. Liu, *Adv. Mater.*, 2011, **23**, 998; (*d*) Y. Sun, X. Hu, W. Luo and Y. Huang, *J. Mater. Chem.*, 2012, **22**, 425; (*e*) Y. Sun, X. Hu,

J. C. Yu, Q. Li, W. Luo, L. Yuan, W. Zhang and Y. Huang, *Energy Environ. Sci.*, 2011, **4**, 2870.
7 (*a*) K. S. Park, S. B. Schougaard and J. B. Goodenough, *Adv. Mater.*, 2007, **19**, 848; (*b*) C. Arbizzani, A. Balducci, M. Mastragostino, M. Rossi and F. Soavi, *J. Power Sources*, 2003, **119–121**, 695; (*c*) L. J. Her, J. L. Hong and C. C. Chang, *J. Power Sources*, 2006, **157**, 457; (*d*) C. Lai, G. Li, Y. Dou and X. Gao, *Electrochim. Acta*, 2010, **55**, 4567; (*e*) L. Zhao, Y. S. Hu, H. Li, Z. Wang and L. Chen, *Adv. Mater.*, 2011, **23**, 1385; (*f*) Y. G. Wang, Y. R. Wang, E. Hosono, K. X. wang and H. S. Zhou, *Angew. Chem., Int. Ed.*, 2008, **47**, 7461.
8 D. Lepage, C. Michot, G. Liang, M. Gauthier and S. B. Schougaard, *Angew. Chem., Int. Ed.*, 2011, **50**, 6884.
9 L. Li, Y. Yu, F. Meng, Y. Tan, R. J. Hamers and S. Jin, *Nano Lett.*, 2012, **12**, 724.
10 (*a*) C. Kvarnström, H. Neugebauer, S. Blomquist, H. J. Ahonen, J. Kankare and A. Ivaska, *Electrochim. Acta*, 1999, **44**, 2739; (*b*) C. Kvarnström, H. Neugebauer, A. Ivaska and N. S. Sariciftci, *J. Mol. Struct.: THEOCHEM*, 2000, **521**, 271; (*c*) P. Damlin, C. Kvarnström and A. Ivaska, *J. Electroanal. Chem.*, 2004, **570**, 113; (*d*) M. J. Ariza and T. F. Otero, *Colloids Surf., A*, 2005, **226**, 270; (*e*) C. Deslouis, T. El. Moustafid, M. M. Musiani and B. Tribollet, *Electrochim. Acta*, 1996, **41**, 1343; (*f*) T. Shimidzu, A. Ohtani and K. Honda, *J. Electroanal. Chem.*, 1988, **251**, 323.
11 (*a*) N. Yamakawa, M. Jiang, B. Key and C. P. Grey, *J. Am. Chem. Soc.*, 2009, **131**, 10525; (*b*) F. Badway, N. Pereira, F. Cosandey and G. G. Amatucci, *J. Electrochem. Soc.*, 2003, **150**, A1209; (*c*) F. Wang, R. Robert, N. A. Chernova, N. Pereira, F. Omenya, F. Badway, X. Hua, M. Ruotolo, R. Zhang, L. Wu, V. Volkov, D. Su, B. Key, M. S. Whittingham, C. P. Grey, G. G. Amatucci, Y. Zhu and J. Graetz, *J. Am. Chem. Soc.*, 2011, **133**, 18828; (*d*) R. E. Doe, K. A. Persson, Y. S. Meng and G. Ceder, *Chem. Mater.*, 2008, **20**, 5274.
12 J. Yan, A. Sumboja, E. Khoo and P. S. Lee, *Adv. Mater.*, 2011, **23**, 746.

